EFFECTS OF COMPRESSIBILITY AND FLUID PROPERTIES IN TURBULENT SUPERSONIC CHANNEL FLOW

Richard Lechner, Jörn Sesterhenn and Rainer Friedrich
Fachgebiet Strömungsmechanik, Technische Universität München,
Boltzmannstr. 15, D-85748 Garching, Germany

ABSTRACT

Direct numerical simulations are performed in nominally fully developed channel flow at global Mach and Reynolds numbers of 1.5 and 3000. A pressure - velocity - entropy form of the compressible Navier - Stokes equations is integrated using a fifth order compact upwind scheme for the Euler part, a fourth order Padé scheme for the viscous terms and a third - order low - storage Runge - Kutta time integration method. Coleman et al.'s (1995) spectral DNS data of turbulent supersonic channel flow in air at $M = 1.5$ and $Re = 3000$ are used to check the accuracy of the method. Excellent agreement is obtained. The present work aims at increasing the insight into effects of compressibility beyond what has been explored by Coleman et al. (1995) and Huang et al. (1995). To this end the nature of fluctuating variables is investigated using scatter plots and transport equations, while the structural effects of compressibility are analysed based on the Reynolds stress budgets and comparisons with their incompressible counterparts. DNS data of turbulent supersonic channel flow in CO_2 at $M = 1.5$ and $Re = 3000$ are used to reveal the effect of thermodynamic properties on mean flow quantities and the turbulence structure.

INTRODUCTION

Fully developed incompressible turbulent channel flow in plane channels has been simulated directly by several authors. DNS data of Kim, Moin, Moser (1987) for low Reynolds number of $Re_\tau = u_\tau h/\nu = 180$ and of Moser, Kim, Mansour (1999) for Reynolds numbers up to $Re_\tau = 590$ are among the most frequently used in investigations of the turbulence structure and attempts to improve statistical turbulence modelling. Since the pressure is no thermodynamic variable in incompressible channel flow, the assumption of fully developed flow is straightforward and in agreement with experimental observations. Compressible channel flow (of ideal gases) which is also driven by a mean pressure gradient, develops downstream, irrespective of the wall boundary conditions, since a decay in pressure implies a decay in density times temperature. In order to allow for streamwise homogeneity in their DNS of turbulent supersonic isothermal-wall channel flow, Coleman et al. (1995) have replaced the mean pressure gradient by a body force which is uniform in streamwise direction, but varies normal to the wall due to the mean density gradient. This variation could have been avoided by replacing the mean pressure gradient by a mean body force $\overline{f}_x$ rather than by $\overline{\rho}\widetilde{f}_x$. Its effect on the turbulence structure, including the Reynolds stress budgets is, however, negligibly small, as has been varified in a separate DNS by Lechner (2000).

Coleman et al.'s (1995) results indicated that the isothermal-wall boundary condition causes a turbulent flow that is strongly controlled by wall-normal gradients of mean density and temperature, to the point that most of the density- and temperature-fluctuations are a result of solenoidal mixing by the turbulence. Hence, the dominant compressibility effect was found to be due to mean property variations so that the van Driest transformation of the mean velocity and a scaling of rms-fluctuations by local values of density and viscosity proved successfull.

Further investigations into intrinsic compressibility effects by Huang et al. (1995) showed that explicit compressibility terms like the pressure-dilatation correlation and the compressible dissipation rate are negligibly small. They confirmed, however, a decay of the turbulent kinetic energy production with respect to the incompressible case and provided a more general representation of the strong Reynolds analogy (SRA) which

matches the DNS data for the cooled channel walls in an excellent way.

This investigation aims at answering some open questions concerning intrinsic compressibility effects in nominally fully developed channel flow at $M = 1.5$ and $Re = 3000$. It concentrates on the role of thermodynamic fluctuations and Reynolds stress balances for two gases, air and CO_2. While the ratio of the specific heats, γ, is 1.4 for air in a large temperature range from $100K$ to $600K$, say, it varies between 1.3 and 1.2 for CO_2 in a similar range, where only translational and rotational degrees of freedom are excited.

A (P, U_I, S)-FORMULATION OF THE NAVIER-STOKES EQUATIONS AND THEIR NUMERICAL INTEGRATION

Using transport equations for pressure and entropy along with the momentum equations has the advantage that two of Kovasznay's 'modes' (Kovasznay (1953)) of compressible turbulence are computed directly. A pressure transport equation is deduced from the continuity equation e.g. replacing material derivatives of density ρ by derivatives of pressure p and entropy s. For thermally perfect gases this leads to:

$$\frac{1}{\rho c^2}\frac{Dp}{Dt} - \frac{1}{c_p}\frac{Ds}{Dt} + \frac{\partial u_j}{\partial x_j} = 0 \qquad (1)$$

$c = (\gamma p/\rho)^{1/2}$ is the speed of sound, γ the ratio of specific heats and $D(...)/Dt$ represents the material derivative following the fluid velocity u_j. Introducing variables of the form

$$X^{\pm} = (u \pm c)\left(\frac{1}{\rho c}\frac{\partial p}{\partial x} \pm \frac{\partial u}{\partial x}\right) \qquad (2)$$

which e.g. describe the propagation of 'waves' in the positive and negative x-direction, Sesterhenn (2001) has cast the compressible Navier-Stokes equations in the following characteristic non-conservative form:

$$\frac{\partial p}{\partial t} = -\frac{\rho c}{2}((X^+ + X^-) + (Y^+ + Y^-) + \qquad (3)$$
$$(Z^+ + Z^-)) + \frac{p}{C_v}\left(\frac{\partial s}{\partial t} + X^s + Y^s + Z^s\right)$$
$$\frac{\partial u}{\partial t} = -\left(\frac{1}{2}(X^+ - X^-) + Y^u + Z^u\right) + \frac{1}{\rho}\frac{\partial \tau_{1j}}{\partial x_j}$$
$$\frac{\partial v}{\partial t} = -\left(X^v + \frac{1}{2}(Y^+ - Y^-) + Z^v\right) + \frac{1}{\rho}\frac{\partial \tau_{2j}}{\partial x_j}$$
$$\frac{\partial w}{\partial t} = -\left(X^w + Y^w + \frac{1}{2}(Z^+ - Z^-)\right) + \frac{1}{\rho}\frac{\partial \tau_{3j}}{\partial x_j}$$
$$\frac{\partial s}{\partial t} = -(X^s + Y^s + Z^s) + \frac{R}{p}\left(-\frac{\partial q_i}{\partial x_i} + \Phi\right)$$

with the abbreviations

$$X^s := u\frac{\partial s}{\partial x}\ ;\ Y^s := v\frac{\partial s}{\partial y}\ ;\ Z^s := w\frac{\partial s}{\partial z} \qquad (4)$$
$$X^+ := (u+c)\left(\frac{1}{\rho c}\frac{\partial p}{\partial x} + \frac{\partial u}{\partial x}\right)\ ;\ X^v := u\frac{\partial v}{\partial x}$$
$$X^- := (u-c)\left(\frac{1}{\rho c}\frac{\partial p}{\partial x} - \frac{\partial u}{\partial x}\right)\ ;\ X^w := u\frac{\partial w}{\partial x}$$
$$Y^+ := (v+c)\left(\frac{1}{\rho c}\frac{\partial p}{\partial y} + \frac{\partial v}{\partial y}\right)\ ;\ Y^u := v\frac{\partial u}{\partial y}$$
$$Y^- := (v-c)\left(\frac{1}{\rho c}\frac{\partial p}{\partial y} - \frac{\partial v}{\partial y}\right)\ ;\ Y^w := v\frac{\partial w}{\partial y}$$
$$Z^+ := (w+c)\left(\frac{1}{\rho c}\frac{\partial p}{\partial z} + \frac{\partial w}{\partial z}\right)\ ;\ Z^u := w\frac{\partial u}{\partial z}$$
$$Z^- := (w-c)\left(\frac{1}{\rho c}\frac{\partial p}{\partial z} - \frac{\partial w}{\partial z}\right)\ ;\ Z^v := w\frac{\partial v}{\partial z}$$

$(u, v, w) = (u_1, u_2, u_3)$ are the cartesian velocity components. The viscous stress tensor τ_{ij} and the heat flux vector q_i are defined by

$$\tau_{ij} = 2\mu s_{ij} - \frac{2}{3}\mu s_{kk}\delta_{ij}\ ,\ q_i = -\lambda\frac{\partial T}{\partial x_i} \qquad (5)$$

$$s_{ij} = \frac{1}{2}\left(\frac{\partial u_i}{\partial x_j} + \frac{\partial u_j}{\partial x_i}\right) \qquad (6)$$

The dissipation rate Φ reads:

$$\Phi = \tau_{ij} s_{ij} \qquad (7)$$

Effects of bulk viscosity are neglected. The thermal equation of state

$$p = \rho R T \quad , \quad R = c_p - c_v \qquad (8)$$

and the following laws for dynamic viscosity μ and heat conductivity λ close the set of equations:

air:

$$\frac{\mu}{\mu_{ref}} = \left(\frac{T}{T_{ref}}\right)^{0.7} \qquad (9)$$

CO_2:

$$\begin{aligned} \mu(T) &= C_1 T + C_2 + C_3/T \qquad (10) \\ C_1 &= 0.2144 \cdot 10^{-7} \quad [Ns/(m^2 K)] \\ C_2 &= 0.2219 \cdot 10^{-4} \quad [Ns/m^2] \\ C_3 &= -0.4387 \cdot 10^{-2} \quad [NsK/m^2] \end{aligned}$$

$$\lambda = \mu \frac{c_p}{Pr} \quad \text{(air, } CO_2\text{)} \qquad (11)$$

The Prandtl number Pr and $\gamma = c_p/c_v$ are kept constant in the temperature range considered.

The advantage of the special form (3, 4) of the Navier-Stokes equations is that boundary conditions can be derived consistently with the equations, without referring to one-dimensional inviscid approximations as proposed by Poinsot and Lele (1992). At an isothermal solid wall lying in the (x, y)-plane, see Figure 1, the unknown wave Z^+ can be computed from equation (3_4).

From eq. (3_1) and Gibbs' fundamental relation the following exact boundary conditions are derived

$$\begin{aligned} Z^+ &= Z^- + \frac{2}{\rho} \frac{\partial \tau_{3j}}{\partial x_j} \qquad (12) \\ \frac{\partial p}{\partial t} &= -\frac{p}{2c} (Z^+ + Z^-) \\ \frac{\partial s}{\partial t} &= \frac{R}{2c} (Z^+ + Z^-) \end{aligned}$$

which show explicitely that p and s evolve in time. Besides this, solid isothermal walls imply

$$\frac{\partial u}{\partial t} = \frac{\partial v}{\partial t} = \frac{\partial w}{\partial t} = \frac{\partial T}{\partial t} = 0 \qquad (13)$$

The special form of the Navier-Stokes equations (3, 4) suggests the use of an upwind discretization of wave-like terms. To this end the compact 5th order upwind scheme 'CULD' (Compact Upwind with Low Dissipation) of Adams and Shariff (1996) has been used. Its resolution properties come close to those of spectral schemes. On the other hand do unsymmetric coefficients generate a small amount of dissipation which is needed to suppress numerical instabilities that may be caused by unresolved high wavenumbers. An explicit filtering of data can thus be avoided. Spatial derivatives appearing in the viscous and heat conduction terms are discretized with an optimized compact 4th order scheme of Lele (1992). The solution is advanced in time with a third-order 'low-storage' Runge-Kutta scheme, proposed by Williamson (1980).

RESULTS

The simulated flows are characterized by the following paramters:

$$M = u_m/c_w \quad , \quad Re = \rho_m u_m h/\mu_w$$

$$Pr = \mu_w c_p/\lambda_w \quad , \quad \gamma = c_p/c_v$$

Their values are:

	M	Re	Pr	γ
air	1.5	3000	0.7	1.4
CO_2	1.5	3000	0.69	1.213

Table 1: Flow parameters.

The computational domain has the size $(L_x, L_y, L_z)=(4\pi, 4\pi/3, 2)h$ in streamwise, spanwise and wall-normal directions, respectively, and is discretized by $(144 \times 80 \times 129)$ points. While the grid is equidistant in (x, y)-directions, the points are clustered close to the wall. The first grid point is at $z_1^+ = z_1 u_\tau/\nu_w = 0.985$ and the tenth at $z_{10}^+ \approx 12.073$. The maximum grid spacing in the core region is $\Delta z^+ = 5.84$.

Fluctuating variables

Figure 2 shows scatter plots of temperature versus density and velocity fluctuations from top to bottom, for air at a position close to the wall (left) and at the centreline (right). Obviously, temperature fluctuations are perfectly correlated with density fluctuations in the wall layer. Conditioned on sweeps (dark grey) and ejections (light grey) they show that sweeps/ejections preferably carry positive/negative temperature fluctuations. The positive correlation between T' and u' is a consequence of wall cooling and associated with non-zero total temperature fluctuations $(T_0'/\overline{T}_0 = O(10^{-1}))$. Scatter plots of entropy fluctuations in Figure 3 show their strong correlation with density and temperature fluctuations near the wall. The fact that s' and p' are decoupled there underlines the lack of intrinsic compressibility and the idea of pure solenoidal mixing in the wall layer. In the core region the level of fluctuations is reduced by nearly an order of magnitude compared to the wall-region, except for the pressure fluctuations which have

the same low level everywhere. Pressure fluctuations behave in a nearly isentropic manner ($p'/\overline{p} = n\rho'/\overline{\rho}, n \approx 1.4889$) in the core region.

Compressibility effects in the Reynolds stress budgets

For brevity we discuss only the budgets of $\overline{\rho u_1''^2}/2$ and $\overline{\rho u_1'' u_3''}$ in Figure 4, i.e. the streamwise and the shear stress components for air. The terms P, TD, VD, M, VPG, DS represent production, turbulent and viscous diffusion, mass flux variation, velocity-pressure-gradient correlation and dissipation. The incompressible data (with symbols) of Kim, Moin, Moser (1987) are included for comparison. All terms have been non-dimensionalized by $\tau_w u_m/h$. The profiles show that the compressibility effect manifests itself mainly in the wall layer where the mean density and temperature have steep gradients. All production, dissipation and redistribution terms are reduced due to compressibility. The compressibility effect is clearly of structural nature.

Effects of fluid properties

Assuming the same wall temperature, Mach and Reynolds number in the DNS of air and CO_2 leads to a decreased bulk velocity and an increased bulk density for the CO_2-flow, compared to the air-flow. This is clear from Figure 5 which contains profiles of mean density and temperature for air and CO_2, normalized with the wall values ρ_w, T_w.

The mean pressure field is nearly unaffected by the change in the ratio of specific heats. The effect of γ on the Reynolds stress tensor and its anisotropy is also weak. The peak rms-density and temperature fluctuations are however reduced by nearly a factor of 2, when γ changes from 1.4 to 1.213. This is a consequence of the reduction in mean density and temperature gradients in the wall layer.

The Reynolds stress budgets for CO_2 show a tendency which is opposite to the previously discussed compressibility effect for air. The production, dissipation and velocity-pressure-gradient terms are slightly enhanced in the wall-layer, but collapse onto their values for air in the core region. This can be interpreted as a damping of the compressibility effect. It also indicates that a change in γ controlls the turbulence structure via the mean density and temperature profiles. Figure 6 displays the budgets of $\overline{\rho u_1''^2}/2$ and $\overline{\rho u_1'' u_3''}$ for air and CO_2.

REFERENCES

Coleman, G. N., Kim, J. and Moser, R. D., 1995, "A numerical study of turbulent supersonic isothermal-wall channel flow", *J. Fluid Mech.*, Vol. 305, pp. 159-183.

Huang, P. G., Coleman, G. N. and Bradshaw, P., 1995, "Compressible turbulent channel flows: DNS results and modelling", *J. Fluid Mech.*, Vol. 305, pp. 185-218.

Kim, J., Moin, P. and Moser, R., 1987, "Turbulence statistics in fully developed channel flow at low Reynolds number", *J. Fluid Mech.*, Vol. 177, pp. 133-166.

Moser, R. D., Kim, J. and Mansour, N. N., 1999, "Direct numerical simulation of turbulent channel flow up to $Re_\tau = 590$", *Physics of Fluids*, Vol. 11, No. 4, pp. 943-945.

Lechner, R., 2000, "Kompressible turbulente Kanalströmung", PH. D. thesis, Technische Universität München.

Kovasznay, L. S. G., 1953, "Turbulence in supersonic flow", *Journal of the Aeronautical Sciences*, Vol. 20, pp. 657-682.

Sesterhenn, J., 2001, "A characteristic-type formulation of the Navier-Stokes equations for high order upwind schemes", *Computers & Fluids*, Vol. 30, No. 1, pp 37-67.

Poinsot, T. J. and Lele, S. K., 1992, "Boundary conditions for direct simulations of compressible viscous flows", *J. Comp. Physics.*, vol. 101, pp. 104-129.

Adams, N. A. and Shariff, K., 1996, "A high–Resolution Hybrid Compact–ENO Scheme for Shock–Turbulence Interaction Problems", *J. Comp. Phys.*, Vol. 127, pp. 27-51.

Lele, S. K., 1992, "Compact Finite Difference Schemes with Spectral-like Resolution", *J. Comp. Phys.*, Vol. 103, pp. 16-42.

Williamson, J. H., 1980, "Low-Storage Runge-Kutta Schemes", *J. Comp. Phys.*, Vol. 35, pp. 48-56.

FIGURES

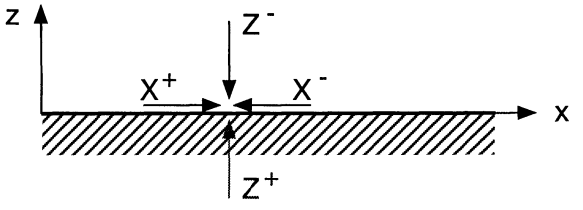

Figure 1: Illustration of boundary treatment at a solid wall.

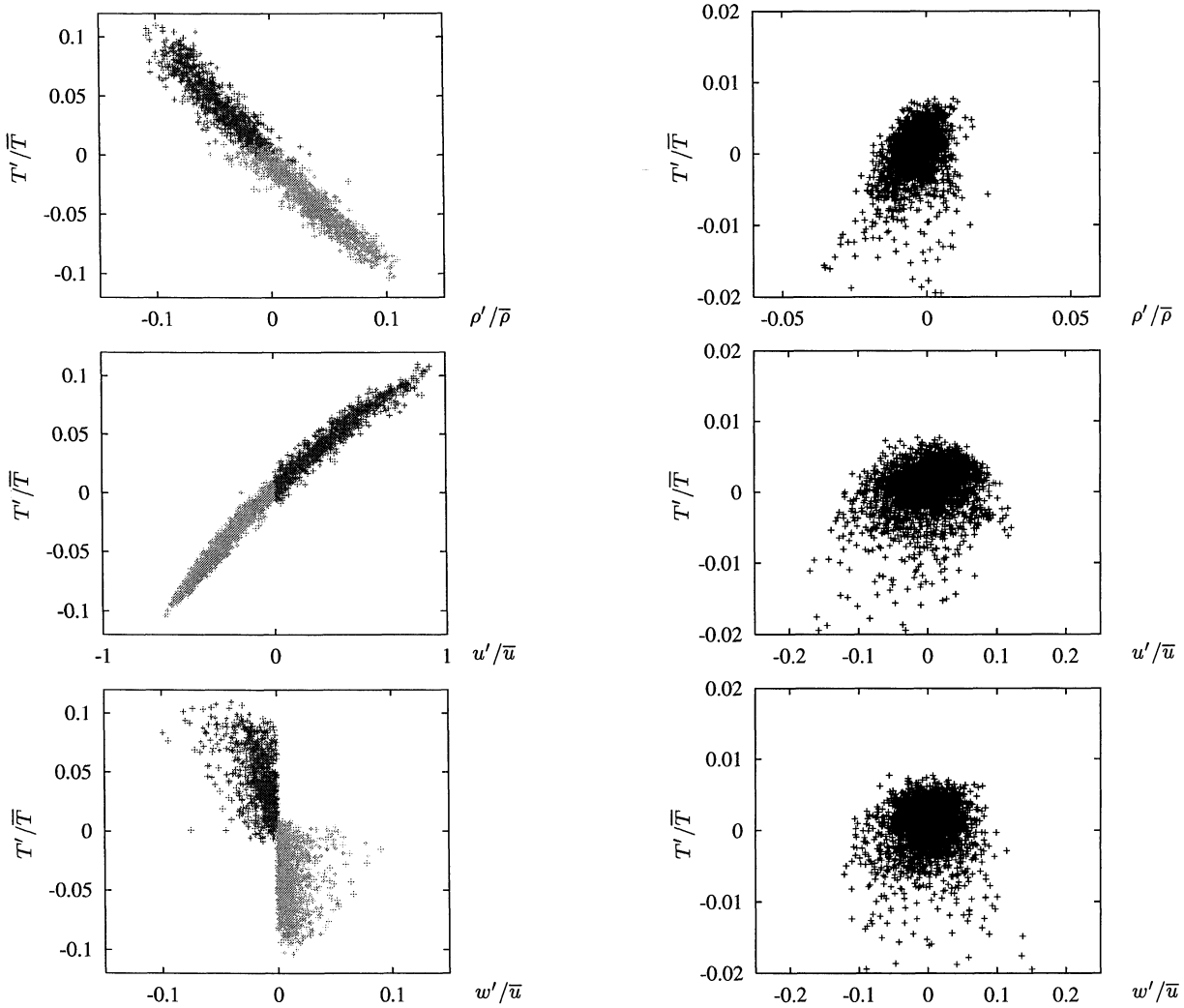

Figure 2: : Scatter plots of temperature versus density and velocity fluctuations in planes parallel to the channel wall at $z^+ = 9$ (left) and in the symmetry plane (right) for air.

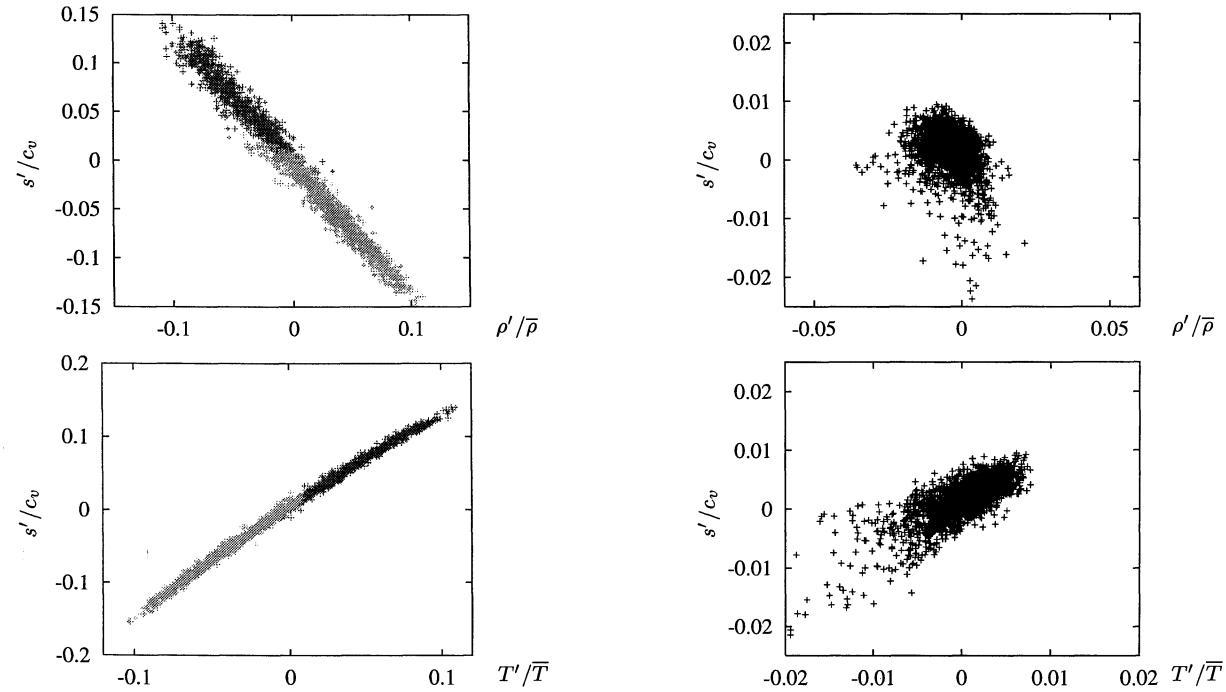

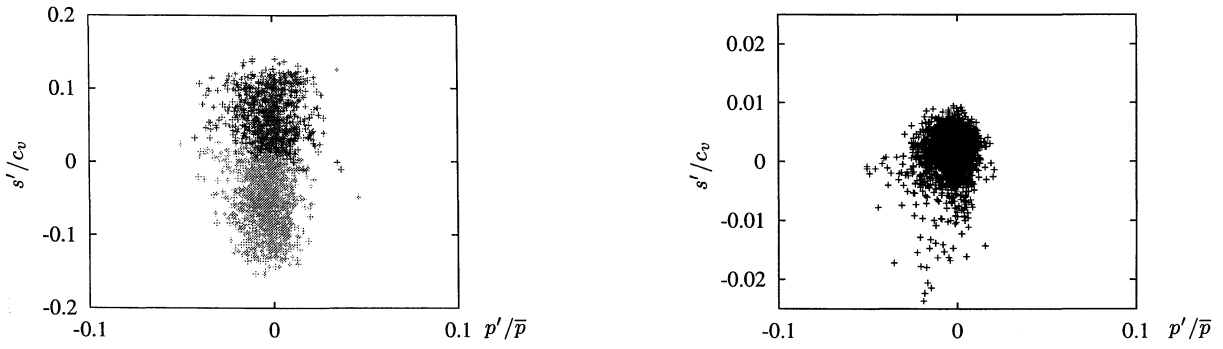

Figure 3: Entropy fluctuations versus density, temperature and pressure fluctuations in planes parallel to the channel walls at $z^+ = 9$ (left) and at the centreline (right) for air.

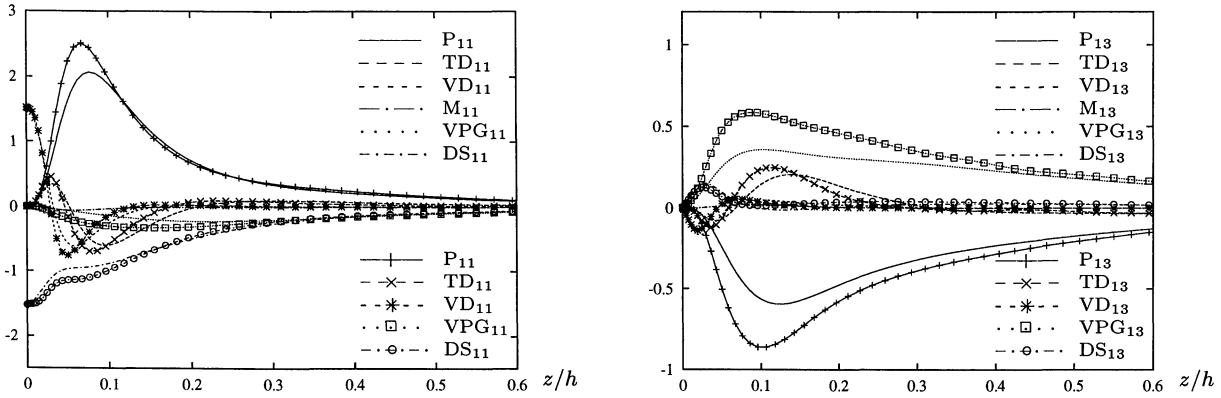

Figure 4: Terms in the budget of $\overline{\rho u_1''^2}/2$ (left) and $\overline{\rho u_1'' u_3''}$ (right) for incompressible ($M = 0$, with symbols) and compressible flow ($M = 1.5$, without symbols) of air.

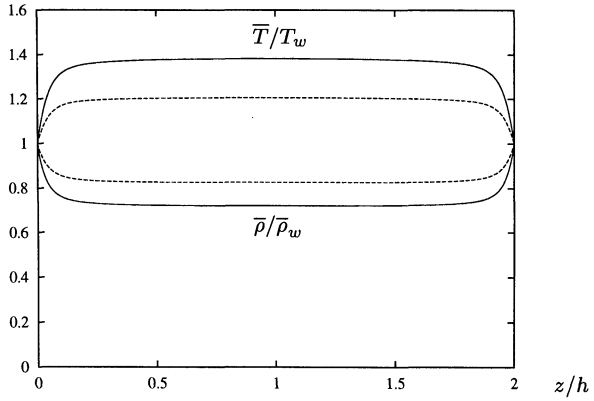

Figure 5: Mean density and temperature profiles for air (green curves) and CO_2 (red curves).

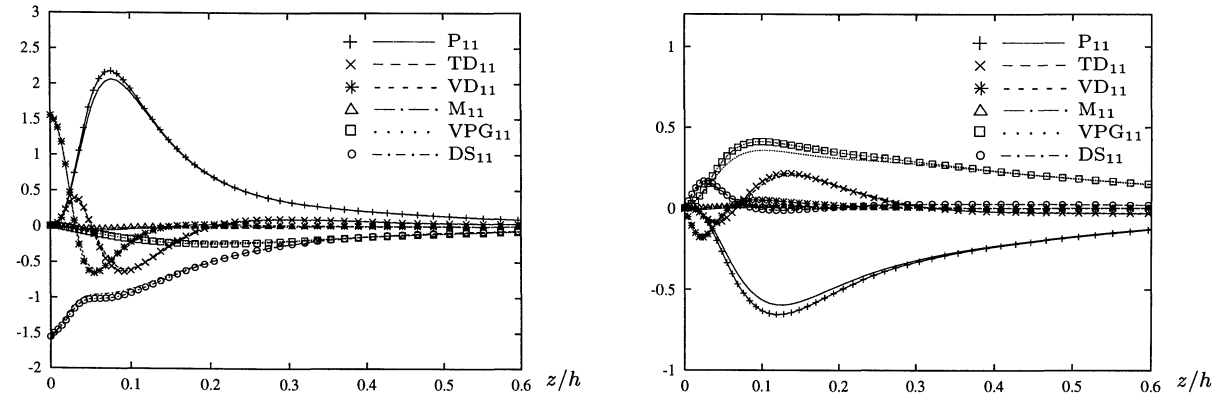

Figure 6: Terms in the budget of $\overline{\rho u_1''^2}/2$ (left) and $\overline{\rho u_1'' u_3''}$ (right) for air (without symbols) and CO_2 (with symbols).